Turk J Elec Eng & Comp Sci, Vol.19, No.2, 2011, © TÜBİTAK
doi:10.3906/elk-1001-374

Cognitive and encrypted communications: state of the art and a new approach for frequency-agile filters

Yahya LAKYS[1], **Balwant GODARA**[2], **Alain FABRE**[1]
[1]*Laboratoire IMS - ENSEIRB, UMR 5218 CNRS, 1 Avenue du Dr. Schweitzer, BP 99, Talence, 33402, FRANCE*
e-mails: yahya.lakys@ims-bordeaux.fr, fabre@ims-bordeaux.fr
[2]*Institut Supérieur d'Electronique de Paris, 28 rue Notre Dame des Champs, Paris, 75006, FRANCE*
e-mail: bgodara@isep.fr

Abstract

Several communication techniques are investigated in the first part of this paper: software radio, cognitive radio and encrypted communications. State of the art of research on agile and reconfigurable filters, passive as well as active, necessary for transceivers is then made and various tables for comparison are given. In the third part, a new theory for a 2^{nd}-order frequency-agile filter is introduced. The center frequency of the filter is proportional to the gain of a feedback amplifier and thus can be tuned over a wide frequency range. This new theory is thereafter generalized to the n^{th}-class leading to a center frequency proportional to $(A)^{n/2}$. Simulation results of band pass agile filters in current mode and made from second-generation current controlled conveyors (CCCII+) in 0.25 μm SiGe BiCMOS technology are given for $n = 1$ and $n = 2$. These simulation results along with results of measurements carried out on the fabricated filters entirely confirm the new approach. They also highlight the improvements to be expected for cognitive and encrypted communications.

Key Words: *Active filters, cognitive radio, current controlled conveyors, frequency agile filters*

1. Introduction

Over the past decades, telecommunications have become an important part of society, in economics as well in terms of technological advances. The convergence of various communication technologies [1–4], necessitates more powerful, multichannel and multifunction terminals leading to several new technologies.

This article presents first a state of the art of these new technologies and their associated techniques: software radio, cognitive radio and encrypted communications. Because analog filtering is one of the most important functions of the associated transmitters-receivers, we will then make successively the state of the art on the various types of frequency agile and reconfigurable filters, as well passive as active, which are likely to be used in these receivers/transmitters.

In the third part, we introduce fully-active frequency-agile filters. This new approach, which concerns band-pass, low-pass and high-pass filters, are generalized to the n^{th}-class and its properties are examined.

Simulations carried out on many configurations of band-pass agile filters made from second-generation current controlled conveyors (CCCII) will then be given to validate this new approach. A corresponding band-pass chip was implemented in a 0.25 μm SiGe BiCMOS technology. The results obtained from on-wafer measurements confirm that this type of filter is a perfect candidate for the realization of frequency agile filters needed for cognitive radio and encrypted communications.

2. Cognitive radio and encrypted communications

2.1. The concept of software radio

Software defined radio, or SDR, is a transmission-reception system whose characteristics (frequency, band-widths, modulation, etc.) are controlled and can be chosen using "computer tools" (software, RAM programmed, etc.) [1, 2]. Such a receiver is called reconfigurable. It is possible to adapt to any frequency, band-width, modulation, etc., corresponding to the standards which were pre-selected. This receiver thus includes a "Hardware" part: electronic circuits of reception; and a "Software" part: control software.

The various electronic functions must thus have sufficiently flexible and powerful characteristics (for example sufficiently broad band-width for a LNA, etc.) in order to be able to satisfy the requirements of the various standards. The various current standards of telecommunication are included in the band 800 MHz–6 GHz [5]. An effective software radio thus must make it possible to cover this range in a continuous way and with the same performances as those required by the already existing standards.

Various approaches are currently used to implement the software defined radio. We analyze them successively as follows.

- For J. Mitola [4], the best way to implement software radio consists, first of all, of digitizing the totality of the spectrum received by the antenna. The signal is then processed: digital filtering of the frequency and the desired channel then demodulated and possibly decoded. This would require obviously a very powerful digital processor. Indeed, a software radio which would work for all current telecommunications standards should cover the frequency range 800 MHz–6 GHz [5]. In order to digitize the signal while respecting the Shannon sampling theorem, it would then be necessary to have a converter ADC of 12 bits functioning for a rate of 12 GS/s (G-Symbols/second) [5, 6]. These performances are well beyond the current state of the art of the converters. Thus, the approach of Mitola does not represent the optimal solution of the realization of the software defined radio.

- The receiver can also be obtained by placing in parallel several elements which correspond to the various standards. One speaks in this case about software radio with traditional multichannel receiver.

  The choice of the elements appropriate to the reception of the selected standard is then carried out using switches. The disadvantage of this solution lies in the high number of elements that it requires, thereby increasing size, cost and consumption.

- Currently the most widespread approach to software defined radio is one using reconfigurable elements. The sharing of certain blocks in the receiver chain makes it possible to reduce the size of the circuit and its consumption. Two reception architectures using reconfigurable elements currently coexist: architecture with direct conversion to "Zero IF" which includes reconfigurable wideband elements and super heterodyne architecture with "digital IF" which includes reconfigurable narrow band elements [7, 8]. Software defined radio, which uses reconfigurable receivers, makes it possible to adapt to any standard of radio communications.

Figure 1 shows the evolution of wireless receivers, from inflexible but easily realizable architectures to entirely flexible but not easily realizable architectures (such as for example that of Mitola) [1]. Current research concentrates on the receivers for which the digitalization of the signal is after RF reception elements, which constitutes a trade-off between two extreme architectures of Figure 1. Such architectures require reconfigurable analog elements: LNA, local oscillators, mixers and filters. Reconfigurable LNA and local oscillators currently exist. As example, broadband LNA [8], make it possible to replace easily several narrow bands LNA, tunable wideband frequency synthesizers were implemented [9]. However, the implementation of integrated and easily reconfigurable RF filters on a wide frequency range remains a more delicate task.

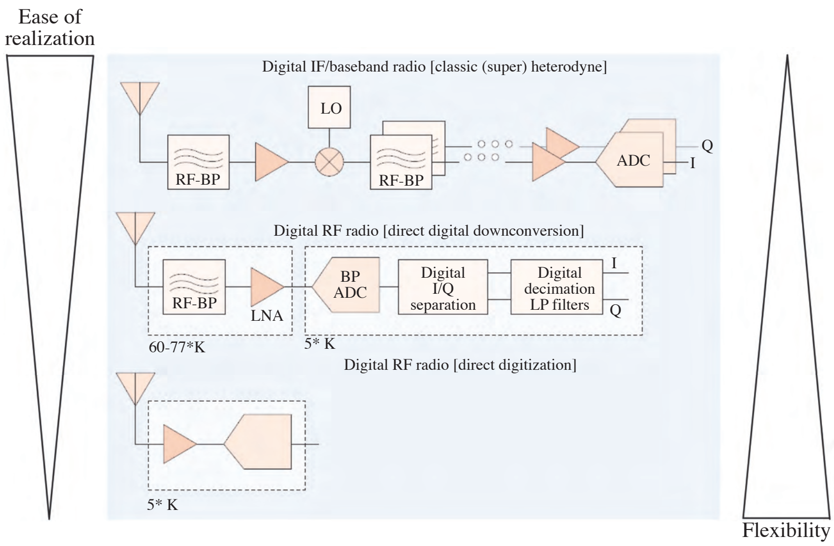

Figure 1. Flexibility versus the ease of realization of various architectures of multichannel reception [1].

2.2. Cognitive radio

Cognitive radio constitutes the most elaborate level of software radio. The term "Cognitive Radio" (CR) was introduced in 1999 by Mitola [10]. Currently, several definitions exist to describe the principles of this system. A CR is an "intelligent" system which is able "to sense its environment" with the aim to determining its characteristics (presence of interferences, noise level, etc.) and to detect the available resources like the wavebands or the presence of prior users. CR must adapt its behavior according to the external parameters which it detected to the needs of its user. It must then act in an autonomous and instantaneous way. The decisions result only from the cognitive software system, without the external intervention of the user [11].

In this way, the dynamic use of the spectrum illustrated in Figure 2 consists of emitting and receiving the signals in the areas of the spectrum which are not occupied at one given moment by other users. The transmitters and the receivers must then adapt their frequencies and signal power in order to ensure a permanent connection under optimal conditions.

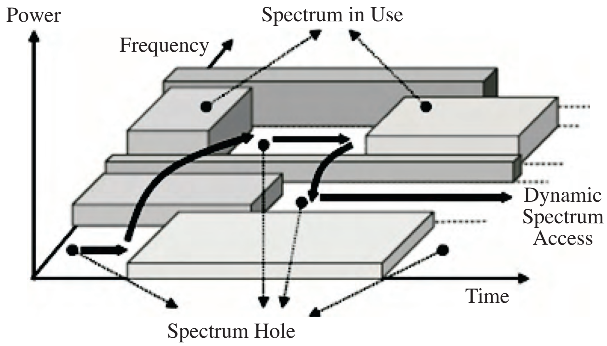

Figure 2. Dynamic access to the spectrum of telecommunications.

Let us notice, however, that these advantages imply transceivers that are both more complex and more difficult to realize. As we mentioned above, cognitive radio includes the concept of the software radio. Indeed, the cognitive radio comprises software functions that allow an optimal reconfiguration. This adaptation of the software radio can be, as we showed, advantageously realized via reconfigurable analog functions. Among those, integrated and reconfigurable RF filters are the most critical functions and most difficult to realize.

2.3. Encrypted communications

Encrypted communications are safe communications for which various techniques of encodings are applied with the basic aim of preventing unauthorized signal reception or making it incomprehensible to undesirable receivers. In order to make these communications not exploitable by an unauthorized receiver, various techniques of encoding are used. The encoding can be done either on the level of information or on the level of frequency [12–14].

The technique of spectrum spreading by frequency hopping (FHSS) consists in transmitting a signal on a band larger than the necessary minimal one [14]. This technique was first introduced with an aim of making military communications safe. It consists in emitting on different carriers. Thus a receiver which does not have the code to synchronize with transmissions will not be able to receive the transmitted signals.

In the state of the art of current military equipment which uses frequency hopping one can quote, HAVEQUIK and SINCGARS [15], for which the frequency hopping or agility range is up to 500 MHz [16].

3. State of the art of reconfigurable filters

The preceding sections showed the interest to use reconfigurable elements for the realization of adaptive receivers. The placement of totally integrated and reconfigurable filters remains a very delicate task. In this section, after making the distinction between adjustable and reconfigurable filters, we will recap the various methods that currently make it possible to produce band-pass adjustable filters (both passive and active).

3.1. Definitions

Several ways of defining the range of adjustment of the center frequency f_0 of the filters are used by various authors. However one among it, that we will adopt, is of most interest to us. By supposing that the center frequency f_0 is adjustable between two values noted $f_{0\,\min}$ and $f_{0\,\max}$, we will call n the ratio [17]:

$$\frac{f_{0\,\max}}{f_{0\,\min}} = n \tag{1}$$

Expression (1) is also often denoted as "n:1." In order to be able to locate well the range of adjustment of f_0 it is also necessary always to indicate the value of $f_{0\,\min}$ or of $f_{0\,\max}$. As an example, we will say that an adjustable filter will have a range n: 1 starting from the frequency $f_{0\,\min}$ when $f_{0\,\max}$ is equal to $n\,f_{0\,\min}$. This definition makes it possible to illustrate the fact that two adjustable filters with a range of adjustment of n:1 are not equivalent if the values of $f_{0\,\min}$ are different (200 MHz and 1 GHz, for example).

3.1.1. Reconfigurability against tunability

In the existing literature, concepts of tunable (or adjustable) and reconfigurable filters are very often used interchangeably. It is thus necessary first of all to establish a definition of the concept of reconfigurability. We can define a "tunable filter" as a filter whose tuning of f_0 is carried out only around f_0 principally to compensate for the drifts (thermal, technological, etc.) while for a reconfigurable filter the variation of f_0 is expected to be carried out over a very wide frequency range.

Thus, we can define now a tunable filter as a filter for which the tuning range is lower than 2:1; i.e. $f_{0\,\max} < 2\,f_{0\,\min}$. Conversely, we will say that a filter is reconfigurable if its tuning range is higher than 2:1, which leads to $f_{0\,\max} > 2\,f_{0\,\min}$.

Let us also specify that to be completely reconfigurable, a filter must have an adjustable quality factor.

3.1.2. Agility

It seems also necessary to define what we understand by agility. A frequency agile filter will be a reconfigurable filter as defined in the preceding paragraph. It must moreover have the property of agility, i.e. the hop between two consecutive frequencies f_1 and f_2 must be able to be carried out very quickly during the transmission of the signal, in order not to disturb the signal processing. Such a filter is perfectly adapted to cognitive radio and encrypted communications.

3.2. Reconfigurable passive filters

Reconfigurable passive filters comprise many possible techniques: integrated LC filters [18–20], SAW and BAW filters [21–23], Ceramic filters [22–27], and planar transmission lines filers [27, 28]. Their reconfiguration is principally made using MEMS and varactors.

Table 1 summarizes the advantages and disadvantages of existing reconfigurable passive filters. It shows that those which occupy a large surface are generally not integrable on silicon; moreover, they only allow limited adjustment of the center frequency f_0. Only ceramic filters allow a higher tuning range, but they require (like transmission line filters) very high biasing, about hundreds of volts. Almost all passive solutions introduce insertion loss.

Table 1. Advantages and drawbacks of existing adjustable passive filters.

Advantages	Drawbacks
Passive filters, adjustment by MEMS	
Low noise Low consumption Very good linearity	High insertion loss (- 14 to -19 dB) Slow switching time (upto 300µs) Big size (some tens of mm²) Need protection for MEMS components (shocks, temperature, moisture…) Problems of reliability of MEMS components Limited frequency tuning range. Analog: up-to 1.26:1 continuous [20] Digital : up-to 1.6:1 discrete [18] In general, low Q-factor
Filters containing components SAW and BAW	
BAW : high Q (order: 1000) BAW : low insertion loss BAW : low consumption BAW : small silicon area BAW : good power handling behavior (for emission, reception)	Adjustment limited, 1 to 2%
Filters containing ceramic components	
Wide frequency tuning range [24] Good selectivity (high Q-factor) Good behavior in power handling. Temperature stability	Important size (>60 mm² [24]) High biasing (order some 100V) Non-integrated with silicon High insertion loss
Filters containing planar transmission lines	
Wide frequency tuning range (3:1) [29]. Good selectivity (high Q-factor) Good behavior in power handling	Big size (>60 mm² [29]) High biasing (hundreds of volts) Non-integrated on silicon High insertion loss

3.3. Reconfigurable active filters

Table 2 summarizes the advantages and the drawbacks of existing adjustable active filters. The partially or entirely active filters are characterized by a reduced size and are easy to integrate on silicon. Also, let us specify that in fact the completely active filters lead to smallest silicon surfaces. They generally present low insertion losses. They present however certain weakness points: their linearity and their entry dynamic range are limited than those of the passive circuits. In addition, the noise of the transistors enhances the inter-modulation product. The consumption of the active circuits is obviously more important than those of the reconfigurable passive circuits.

3.4. Comparison of the characteristics of the various reconfigurable filters

From the preceding state of the art, we represent on Figure 3 the classification which one can carry out for the various types of reconfigurable filters which currently exist. For each type of filter is indicated on the first line the technology, topology or the active element used (according to the case). On the second line the element through which the adjustment of the filter parameters is carried out.

Table 2. Advantages and drawbacks of existing adjustable active filters.

Advantages	Drawbacks
Partially Active Filters, LC with Varactors	
reduced size compared to the external passive filters Easily integrated on silicon	Low Q for integrated inductors(order of 5) Need for an active circuit for Q improvement (source of noise and non- linearity) Low tuning range of f_0 (up-to 1.4:1 [30]) Power consumption
Partially Active Filters, LC with OTA	
Reduced size compared to the external passive filters Easily integrated on silicon Q up to 350 [31]	Low tuning range of f_0 1.25:1 [31] Limitation because of the performances of OTA Power consumption
Entirely Active Filters : Variables State	
Ease of realization Availability of all the transfers (LP, BP, HP)	limited performance, low frequency (up to 10MHz) Power consumption
Entirely Active Filters : Switched capacitor	
Integrated on silicon High quality factor of (up to 300 [32]) Small surface <2mm² [27]	Discrete time Need for a clock at high frequency Low tuning range (up-to 2.2:1 [32]) Frequency Limitation (up-to 530MHz [32]) Power consumption
Entirely Active Filters : Simulation of inductor	
reconfigurable filters having the most reduced sizes wide band of adjustment : 3:1 [33] Ease of adjustment (Biasing currents) High quality factor up to 140 338] or 300 [34]	Power consumption

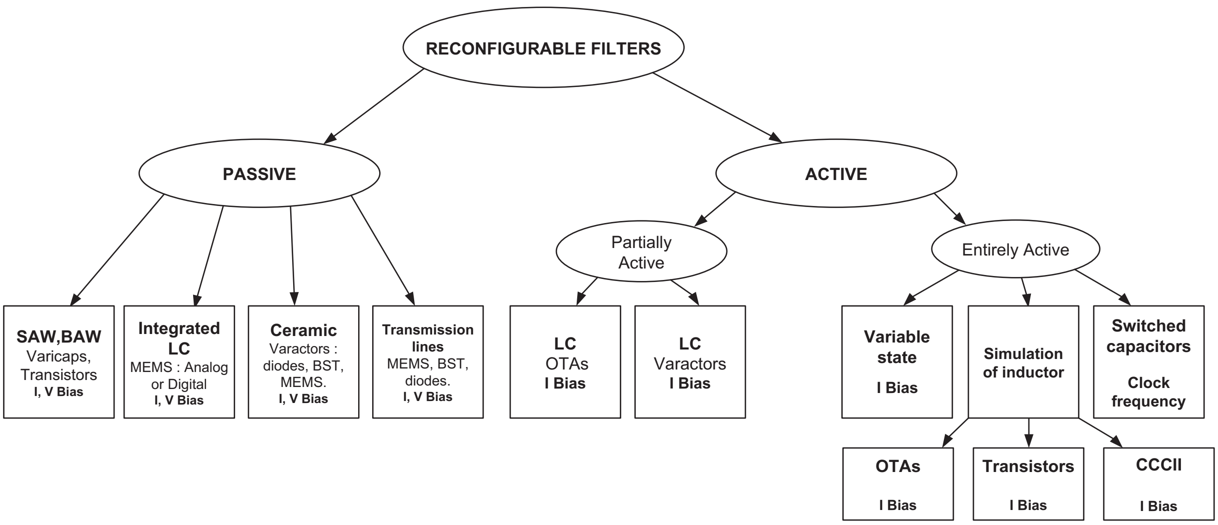

Figure 3. Proposed general classification for the existing reconfigurable filters.

After having carried out the classification of the various reconfigurable filters, it is necessary to compare their possibilities. We have indicated the principal properties of the various kinds of adjustable filters on Table 3. This table confirms that the passive filters (entirely or partially) are those which occupy the most important silicon area (always higher than 1 mm^2). The entirely active filters on the other hand occupy a reduced surface which is about some μm^2 it is thus at least 1000 times smaller than that of the passive filters.

The table indicates the state of the art for each type of filter met as well as the corresponding reference. We first of all showed the most important parameters for the agility: maximum center frequency, f_0 tuning range (also characterized by value n:1), switching time of f_0, the quality factor and the necessary silicon surface. The table mentions also the consumption magnitude, the dynamic range and the insertion loss. Generally, it is noted that when $f_{0\,\max}$ is high (>1 GHz) the value of n remains lower than 2, except for the ceramic filters. For the latter, surface (of silicon) is higher than 10 mm^2, the control voltage is important (> 100 V, see table 1) and the f_0 switching time is very high. The only filters for which the switching time of f_0 is compatible with the agility (filter) are those tuned by active elements and the switched capacitor filters. SAW and BAW filters have the highest quality factors.

Table 3. Comparison of the characteristics of the various kinds of reconfigurable filters.

Topology of the filter			reconfiguration Technique	f_{0max} (GHz)	Maximum value of n @ $f_0$min	Switching time of f_0	Q	Size	Consumption	Linearity and Dynamic range	insertion loss
PASSIVE FILTERS	LC		By MEMS: -analog -digital	3 [29]	1.26:1 @ 1.87 GHz [20] (continuous) 3:1 @ 25 MHz [35] (discrete)	1-300µs	High, more than 800 [29]	Very large 10mm²	-low -High biasing voltage	Important	High
PASSIVE FILTERS	SAW, BAW		-Varicaps -Transistors	6 [36]	1 to 2% [36]	1-100ns	1000	Large 1mm²	-Very low : adjustment circuit	High	Medium
PASSIVE FILTERS	Ceramics		By Varactors: -with semiconductor (diodes) -with dielectric (BST) -Mechanical (MEMS)	2.4 [24]	3:1 @ 800 MHz [24] (continuous)	1-300µs	800	Very large 10mm²	-low : adjustment circuit -High biasing voltage	High	High
PASSIVE FILTERS	Coplanar transmission lines (CPW)		Variation in the-length of the line: -geometrical by MEMS, -electric by BST or diodes	18 [37]	1.5:1 @ 12 GHz [37] (discrete) 4:1 @ 350 MHz [29] (discrete)	1-300µs	-	Very large 72mm²	Very low : Tens of µW	Important (IIP3 41dBm)	High
ACTIVE FILTERS	Partially	LC	-Varactors -OTA	2.5	1.39:1 @ 1.8 GHz [30] 1.25:1 @ 1.6 GHz [31]	1-100ns	100 [38]	Very large >8 mm²	High > 54 mW	SFDR > 30dB	Low
ACTIVE FILTERS	entirely	Variable state	-Biasing current	-	-	1-100ns	-	-	-	-	Low
ACTIVE FILTERS	entirely	Switched capacitors	-Frequency of clock	0.6 [32]	2.2:1 @ 240 MHz [32]	1-100ns	Up to 300	Large 1mm²	High 60 mW [32]	DR. > 30dB	Low
ACTIVE FILTERS	entirely	With active inductor	-Biasing current	1.56 [34]	1.53:1 @ 1.6 GHz [39] 2.75:1 @ 400 MHz [40]	1-100ns	Up to 300 [37]	Very low < 0,03 mm² [41]	High 46 mW [33]	DR. = 54dB [42]	Low

The consumption of the active filters is greater. It however in general remains always lower than 100 mW. The passive filters are generally characterized by a better linearity. However, their insertion losses are higher than for the active filters.

4. A New approach for frequency-agile active filters

The implementation of the frequency agile filter is based on a classical second order filter structure which includes an input and two different outputs at least: band-pass and low-pass. This idea was first initiated in 1996 [43].

In the following sections, we will introduce the new theory making use only of voltage mode circuits, however it is obvious that the agile filters may also be obtained from circuits operating in current mode.

4.1. Description of the basic second order cell

Figure 4 shows the classical second order filtering circuit operating in voltage mode. It includes at least both a band-pass and low-pass outputs. This cell that will be called class 0 filter constitutes the basic element for the implementation of a frequency agile filter.

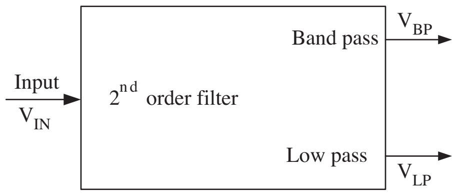

Figure 4. Basic second order filter including two different outputs.

V_{in} is the input voltage of the filter. V_{BP} and V_{LP} are, respectively, its band pass and low pass outputs. The transfer functions $F_{BP}(s)$ and $F_{LP}(s)$ are, respectively, given by the following relations:

$$F_{BP}(s) = \frac{V_{BP}}{V_{IN}}(s) = \frac{a' s}{1+as+bs^2} \tag{2}$$

$$F_{LP}(s) = \frac{V_{LP}}{V_{IN}}(s) = \frac{d'}{1+as+bs^2}. \tag{3}$$

In these equations, a and b are real positive constants to ensure stability of the filter. We also suppose that a' and d' are real positive constants. The values of these constants are related to the values of the different components of the circuit in Figure 4. They allow us to determine the characteristic parameters of the filter.

Its center frequency is given by $f_0 = 1\Big/2\pi\sqrt{b}$. This frequency corresponds simultaneously to the center frequency of the band-pass and the -3dB cutoff frequency for the low-pass output. The quality factor is given by$Q = \sqrt{b}\Big/a$. The gain at f_0 of the band pass is $G_{BP} = a'/a$, and its -3dB Bandwidth is $\Delta f = a/2\pi b$. The gain at low frequency for the low pass output is $G_{LP} = d'$. Generally for a conventional filter, the gains of the two outputs will be greater than or equal to unity, i.e. $a' \geq a$ and $d' \geq 1$.

4.2. Block diagram of the new frequency agile filter

Figure 5 shows the new second order frequency agile filter circuit obtained from the previous basic cell. It will be called class 1 frequency agile filter. The voltage of the low pass output is first amplified through an amplifier with an adjustable gain A. The amplified voltage is then added to the input voltage V_{IN} of the previous circuit.

The new input voltage of the filter is then V_E and the circuit always includes two outputs: V_{LP} and V_{BP} which remain of the same type as the starting structure.

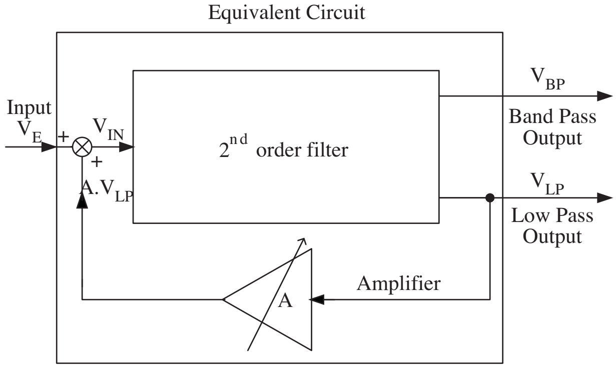

Figure 5. Frequency agile filter made from the basic cell.

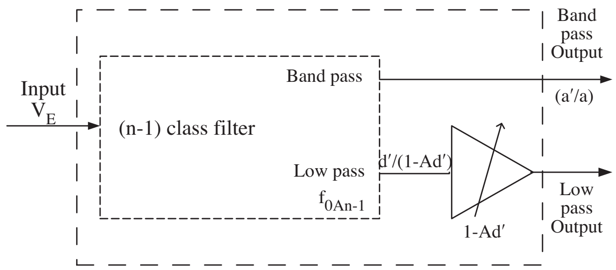

Figure 6. Necessary modifications of the (n-1)th class agile block.

4.3. Expression of the transfer functions

The input signal of the new circuit is now given by the formula $V_E = V_{IN} - A \cdot V_{LP}$. As shown by the following calculations, output V_{BP} remains band-pass. Its corresponding transfer function $F_{BP}(s)$ is then

$$F_{BP}(s) = \frac{V_{BP}}{V_E}(s) = \frac{\frac{a's}{(1-Ad')}}{1+\frac{as}{(1-Ad')}+\frac{bs^2}{(1-Ad')}}. \tag{4}$$

This is a band pass function whose voltage gain, $G_{BPA} = \frac{a'}{a}$, remains identical to the gain of the starting band-pass in Figure 4.

The output V_{LP} of the new filter also remains of the same type as for the starting filter. It's a low pass output. Its new transfer function becomes

$$F_{LP}(s) = \frac{V_{LP}}{V_E}(s) = \frac{\frac{d'}{(1-Ad')}}{1+\frac{as}{(1-Ad')}+\frac{bs^2}{(1-Ad')}} \tag{5}$$

Its voltage gain is

$$G_{LPA} = \frac{d'}{(1-Ad')}. \tag{6}$$

The characteristic frequency f_{0A} of this new circuit is then given by

$$f_{0A}=\frac{\sqrt{(1-Ad')}}{2\pi\sqrt{b}}, \tag{7}$$

And its Q-factor becomes

$$Q_A=\sqrt{(1-Ad')}\cdot\frac{\sqrt{b}}{a} \tag{8}$$

The Expressions (7) and (8), which allow us to determine the bandwidth of the band-pass output, show that it remains the same as for the circuit in Figure 4, $\Delta f_A = \Delta f$.

Table 4 summarizes the characteristics of the two circuits: starting filter in Figure 4 an agile filter in Figure 5. The center frequency of the agile filter (Figure 5) is related to the center frequency f_0 of the starting filter through a coefficient that depends both on A (Gain of the amplifier) and d', gain of the starting low-pass (Figure 4). The gain of the band-pass remains unchanged, while the gain of the low-pass is divided by 1-Ad' and is subsequently lower than the gain in the starting circuit. This table also shows that the -3 dB bandwidth of the band-pass output remains unchanged for the circuits in Figure 4 and 5. Equation (4) and (5) indicate that the new circuit will be stable provided that 1-Ad' remains positive (Routh-Hurwitz criterion) [44].

Table 4. Characteristic parameters of the filters in figures 4 and 5.

	Basic Circuit (Figure 4)	Frequency agile filter (Figure 5)
Center frequency	$f_0=\frac{1}{2\pi\sqrt{b}}$	$f_{0A}=\sqrt{(1-Ad')}\cdot f_0$
Q-factor	$Q=\frac{\sqrt{b}}{a}$	$Q_A=\sqrt{(1-Ad')}\cdot Q$
BP Gain	$G_{BP}=\frac{a'}{a}$	$G_{BPA}=G_{BP}$
BP : -3dB Bandwidth	$\Delta f=\frac{a}{2\pi b}$	$\Delta f_A=\Delta f$
LP Gain	$G_{LP}=d'$	$G_{LPA}=\frac{G_{LP}}{(1-Ad')}$

4.4. Generalization: frequency agile filter to the class n

4.4.1. Modification of the circuit to the class n-1

A voltage amplifier of gain 1-Ad$'$ must be added to the low-pass output of the filter to class n-1 in order to meet the same conditions of the stating block (Figure 4). This modified circuit is shown in Figure 6.

4.4.2. Configuration of the nth-class agile filter

In the same way as the above transformations, an amplifier with tunable gain A is added to the low-pass output, the amplified voltage is then added (as for the circuit in Figure 5) to the input voltage V_{in} (Figure 7).

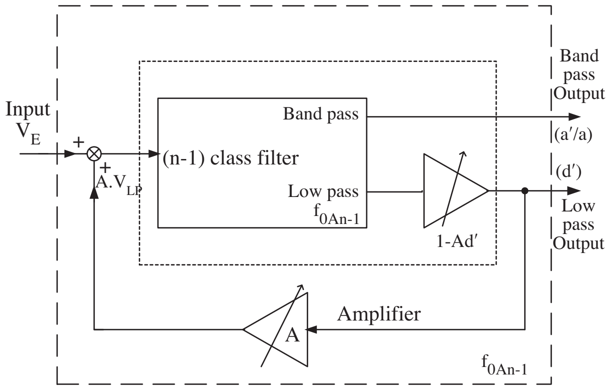

Figure 7. Class n frequency agile filter.

4.4.3. Properties of the nth-class agile filter

In the various transformations that have been successively applied, it is noticeable that only two types of adjustable-gain amplifiers are used: amplifiers with gain A and amplifiers with gain 1-Ad', with $A < 1/d'$. This last condition is necessary to ensure the stability of the circuits.

The different characteristic parameters of the nth-class agile filter according to those of the starting block (Figure 4) are given in Table 5. The constants a, b, a' and d' were defined in section 4.1.

Table 5. Characteristic parameters of the nth-class agile filter (Figure 7) and the zero-class filter (Figure 4).

	Starting Block (Figure 4)	nth-class frequency agile filter (Figure 7)
Center frequency	$f_0 = \frac{1}{2\pi\sqrt{b}}$	$f_{0An} = \sqrt{(1-Ad')} \cdot f_{0An-1} = (1-Ad')^{\frac{n}{2}} f_O$
Q-factor	$Q = \frac{\sqrt{b}}{a}$	$Q_{An} = \sqrt{(1-Ad')} Q_{An-1} = (1-Ad')^{\frac{n}{2}} Q$
BP Gain	$G_{BP} = \frac{a'}{a}$	$G_{BPAn} = G_{BP}$
BP : -3dB Bandwidth	$\Delta f = \frac{a}{2\pi b}$	$\Delta f_{An} = \Delta f_{An-1} = \Delta f$
LP Gain	$G_{LP} = d'$	$G_{LPAn} = \frac{G_{LP}}{(1-Ad')}$

The equation linking the final frequency f_{0An} to the frequency f_0 of the starting block (Table 5) will allow us to study the variation of f_{0An} according to the parameter n and the gain A of the amplifier. This variation is shown in Figure 8. The term $\sqrt{(1-Ad')}$ in the equation of f_{0A} and Q_A leads us to consider several possible cases depending on the sign and the value of $(1-Ad')$. When we set the values of the starting constants a, b, a' and d' that we have assumed positive, we must distinguish three possible cases, according to the sign and the value of A. These cases are represented in Figure 8 by three regions that give the value of the ratio f_{0An}/f_0 depending on the gain A of the amplifier.

- For region 1 in which $\mathbf{1-Ad'} <$ i.e. $\mathbf{A > 1/d'}$, the gain of the amplifier is positive and greater than $\mathbf{1/d'}$. The agile filter will not then be able to operate because the factor $\sqrt{(\mathbf{1-Ad'})}$ is not real positive.

- For region 2 in which $\mathbf{0 < 1 - Ad' < 1 \Rightarrow 0 < A < 1/d'}$, the gain of the amplifier is positive and lower than $\mathbf{1/d'}$. The stability conditions are ensured and the filter can operate here correctly. The factor $\sqrt{1-Ad'}$ being lower than unity, it results that the center frequency $\boldsymbol{f}_{0An}$ of the circuit in Figure 5 is then lower than the center frequency f_0 of the starting filter.

- For region 3 in which $\mathbf{1 - Ad' > 1 \Rightarrow A < 0}$, the gain of the amplifier is negative. The center frequency f_{0An} of the circuit in Figure 5 is greater than the center frequency f_0 of the starting filter. This case seems to be the most interesting one.

This figure also illustrates the linear shape of the ratio for $n = 2$. It also indicates that when A is negative the variation of f_{0An}/f_0 will be faster as much as n will be greater.

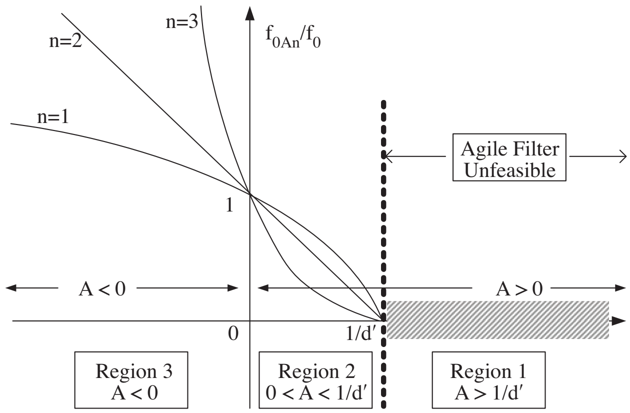

Figure 8. Variation of f_{0An}/f_0 as a function of A for various values of n.

4.4.4. Particular case

In the general study the parameter d' is the voltage gain of the low-pass output of the starting block (filter at class 0, Figure 4). When the value of d' is chosen equal to unity. All the above circuits are simplified because the only required amplifier gains are A and 1-A. In current mode for example, these two values can be achieved easily from only one amplifier with gain A.

4.5. Sensitivity of the filter parameters

As shown in table 5 the modification of the amplifier gain A allows tuning of the center frequency f_{0An} of the agile filter. Once the center frequency is set, an accidental variation of small magnitude of A would bring the lowest possible variation on f_{0A}. These effects are characterized by studying the corresponding sensitivities. The general equations in Table 5 allow us to determine the sensitivities of the different parameters according to the gain A and to n. The expressions of the different sensitivities are

$$S_A^{f_0An} = S_A^{Q_{An}} = \frac{-n}{2} S_A^{G_{LPAn}} = \frac{-nAd'}{2(1-Ad')} \tag{9}$$

$$S_A^{G_{BPA}} = S_A^{\Delta\omega An} = 0. \tag{10}$$

Figure 9 shows the variation of $S_A^{f_{0An}}$ according to gain A and parameter n. This sensitivity increases with n. Its magnitude becomes significant when A tends to $1/d'$ or when A is negative and have a high magnitude. Generally, when A is negative and its magnitude is high, $S_A^{f_{0An}}$ tends to $n/2$. Also note that, when $n=2, S_A^{f_{0An}}$ is always less than unity when A is negative. When A is positive, its magnitude should stay less than $1/2d'$ to have the sensitivity lower than unity. Under these conditions, $A \leq 1/2d'$, the frequency agile filter would be insensitive because a variation of A about 1% brings a relative variation on f_{0An} about 1%. Equations (9) to (10) show also that the same is true for Q and for the gain of the low-pass filter G_{LPA}. The variation of A is furthermore without incidence on the bandwidth $\Delta\omega$ and the gain of the band-pass.

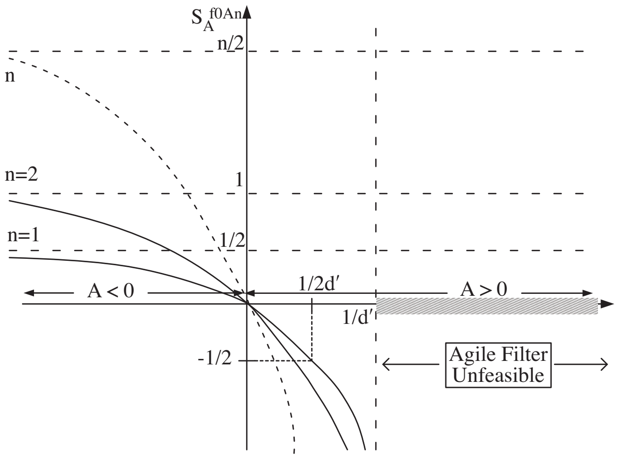

Figure 9. variation of $S_A^{f_{0An}}$ as a function of A for various values of n.

5. Validation circuits

5.1. General information

The theory that we have introduced in voltage mode is also valid in current mode. Voltage mode is traditionally used while current mode is generally preferred for applications at high frequencies [45]. Furthermore, when a function requires many signals summing, the current mode will be preferred too because the current sums can be done on the nodes without requiring additional circuits. For all these reasons, we have implemented our validation circuits in current mode using second-generation current controlled conveyors (CCCII+) [33, 46]. This circuit operates in class AB. Figure 10 shows its associated symbol. Its matrix relationship between conventional variables is then [33, 46]

$$\begin{pmatrix} i_y \\ V_x \\ i_{Z+} \end{pmatrix} = \begin{pmatrix} 0 & 0 & 0 \\ 1 & R_X & 0 \\ 0 & 1 & 0 \end{pmatrix} \begin{pmatrix} V_y \\ i_x \\ V_{Z+} \end{pmatrix}. \tag{11}$$

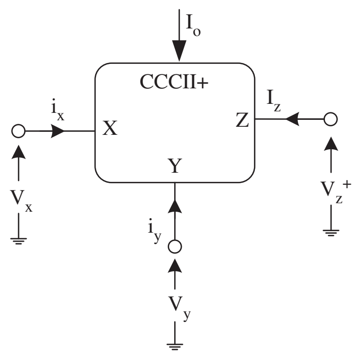

Figure 10. Current controlled conveyor (CCCII+), associated symbol. Its intrinsic resistance on X is $R_X = V_T/2I_0$.

5.2. Zero-class circuit

Figure 11 shows the starting second order filter (that we call filter to the class 0, n=0). The circuit includes three current controlled conveyors with positive current transfer from X to Z (CCCII+). The section conveyor (1, 2), capacitor $C1$ and capacitor $C2$ is equivalent to a shunt RLC circuit. The conveyor (Q), connected as a negative resistance [45], allows tuning of the quality factor of the filter through the bias current I_Q. This filter has a band-pass output I_{OUT} whose gain is $-R_{X2}/\left(R_{X1}+R_{X2}-R_{X1}R_{X2}/R_{XQ}\right)$. Its transfer function is

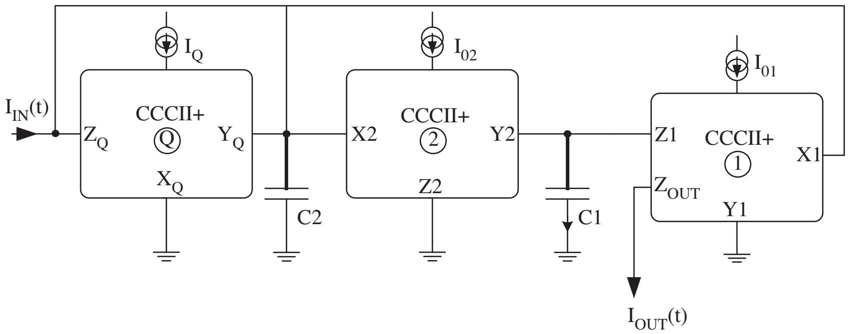

Figure 11. Starting second order filter (zero-class filter).

$$\frac{I_{OUT}}{I_{IN}}\left(s\right)=\frac{-R_{X2}C_1 s}{D(s)}, \tag{12}$$

with $D\left(s\right)=1+\left[R_{X1}+R_{X2}-\frac{R_{X1}R_{X2}}{R_{XQ}}\right]C_1 s+R_{X1}R_{X2}C_1C_2 s^2$.

The voltage across capacitor C1 has a low-pass transfer function that makes it possible to have the amplified feedback current that is added to the initial input current (see Figure 5):

$$\frac{V_{C1}}{I_{IN}}\left(s\right)=\frac{R_{X2}}{D(s)}. \tag{13}$$

The center frequency of the filter is f_0=$1/2\pi\sqrt{R_1R_2C_1C_2}$. When the currents I_{01} et I_{02} are chosen to be identical to I_0 (i.e. $R_{X1}=R_{X2}=R_X$) and the capacitors C1 and C2 are identical, *C1 = C2 = C,* the characteristic expressions of the filter are

$$f_0=\frac{1}{2\pi R_X C} \tag{14}$$

$$Q=\frac{R_{XQ}}{2R_{XQ}-R_X}. \tag{15}$$

The filter is orthogonal, the bias current I_0 allows through R_X, but to some extent only, to change f_0. The current I_Q, through R_{XQ}, makes it possible to tune Q to the desired value. The gain of the band pass output is then $-R_{XQ}/(2R_{XQ}-R_X)$. The previous equation for Q shows that the stability of the filter implies that $2R_{XQ}$ exceeds R_X, i.e. that I_Q must be less than $2I_0$.

5.3. Class 1 frequency agile filter

Figure 12 shows the corresponding agile filter to class 1, ($n = 1$), which is directly deduced from the theory that we have introduced in the previous sections. This filter corresponds to the case of negative A. The gain A is done by the conveyor (CR). The expression of the feedback amplified current that is added to the input (see Figure 5) is V_{C1}/R_{XCR}. Where $R_{XCR} = V_T/2I_{0CR}$ is the intrinsic resistance of the input X of CCCII (CR). The gain A of the amplifiers, with $|A| = I_{0CR}/I_0$, can then be directly changed by the biasing current I_{0CR} of this conveyor. In this case (A<0) the center frequency f_{0A1} will be higher than the starting center. It is given by: $f_{0A1} = \sqrt{(1-A)}f_0$. The band pass output of the filter is I_{out}.

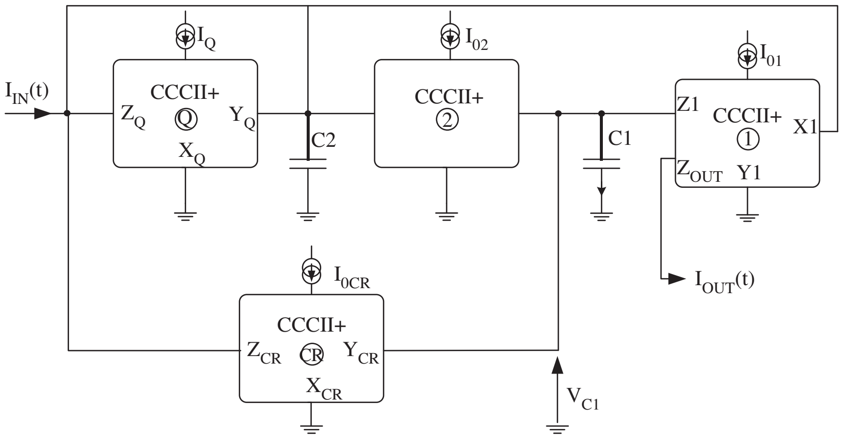

Figure 12. Class 1 frequency agile filter with $A < 0$, deduced from circuit in Figure 11.

In order to obtain a center frequency lower than f_0 (corresponding to the case $A>0$, Figure 6), we could replace conveyor (CR) by another CCCII with negative current transfer from X to Z (CCCII-).

5.4. Class 2 frequency agile filter

Figure 13 shows the corresponding agile filter at the class 2 for negative values of A. The different feedbacks are also achieved here from a single current conveyor (CR). The gain A is always related to I_{0CR}/I_0. To that conveyor, additional Z outputs were added. The corresponding gain of each output is clearly indicated on its symbol. The output Z with gain $|A|$ ($i_z/i_x = |A|$) was obtained by properly dimensioning the emitter areas of the transistors of this output.

Note that the joint use of the current mode and CCCII cells allows us to obtain a 2^{nd}-class agile filter implementation having no more active elements than the 1^{st}- class agile one in Figure 12.

The band pass output remains I_{OUT} and the center frequency is given here by the relation

$$f_{0A2} = (1 - A)\, f_0. \tag{16}$$

This output current is obtained at high impedance. Thus, various elementary cells of Figure 13 can be connected in cascade without requiring any additional stage.

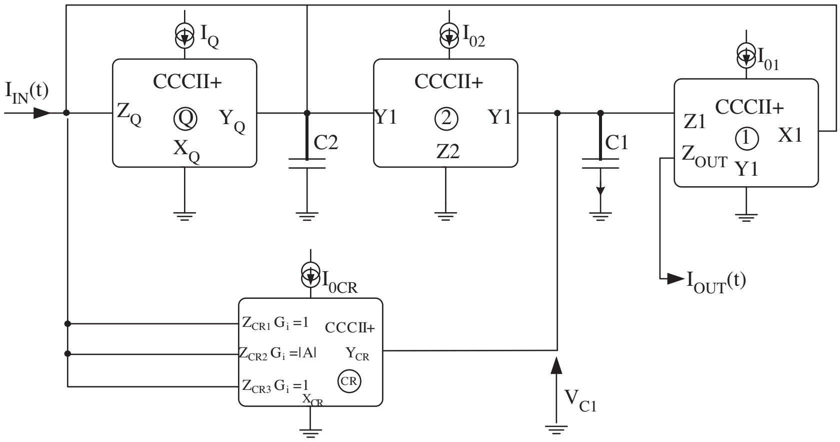

Figure 13. Class 2 frequency agile filter with A < 0, deduced from circuit in Figure 12.

5.5. Simulation results

The different circuits were integrated in 0.25 μm SiGe BiCMOS technology from STMicroelectronics [47]. The transition frequency of the NPN transistors in this technology is 55 GHz; the vertical PNP transistors have f_{TP} of 6 GHz. The characteristics of the CCCII in this technology are given in table 6, for ± 2.5 V and I_0 = 100 μA.

Table 6. characteristics of the CCCII, $V^+ = -V^- = 2.5$ V; $I_0 = 100$ μA.

	Voltage follower	Current follower
Gain (dB)	-0.009	0.03
-3 dB Bandwidth	21.6 GHz	4.5 GHz
Input Impedance	466 kΩ//0.046 pF	162 Ω
Output Impedance	162 Ω	152k Ω//0.04 pF
Output offset	486 μV	3 μA
Consumption	2.57 mW	2.57 mW

Figure 14(a) shows the frequency responses at f_{0A1} = 391 and 541 MHz of the band-pass output obtained by simulations of the class 1 agile filter with $I_{01} = I_{02} = I_0 = 50$ μA and $V+ = V- = 2.5$ V and when the gain is changed by biasing current I_{0CR} ($I_{OCR}/I_0 = |A|$). The corresponding power consumptions are respectively: 8 and 14.5 mW. We have also showed the frequency response, at f_0 = 239 MHz, of the starting filter (class 0).

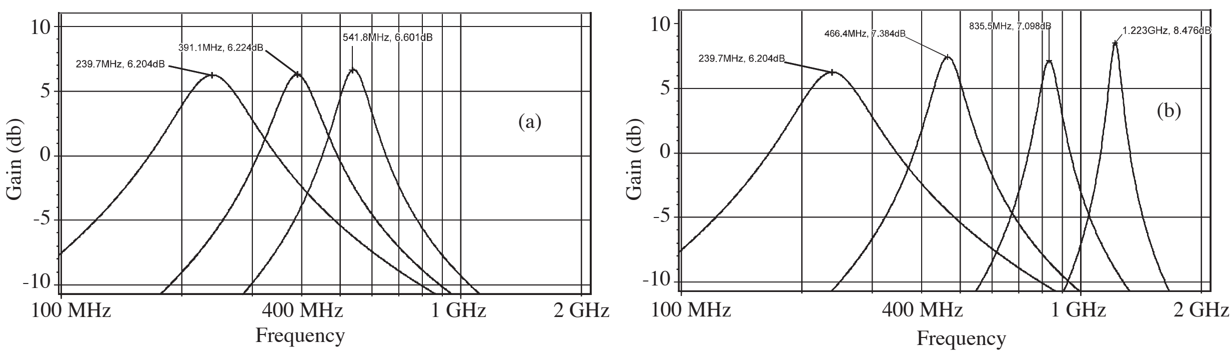

Figure 14. Simulated frequency responses of the agile filters: (a) 1^{st}-class, (b) 2^{nd}-class.

Similarly, the frequency responses $f_{0A2} = 466, 835$ MHz and 1.22 GHz obtained under the same conditions for the class 2 agile filter are shown in Figure 14(b). the corresponding power consumptions are respectively here 7.1, 11.3 and 20.1 mW.

Figure 15 shows the evolution of the theoretical and simulated frequencies f_{0A1} and f_{0A2} for both 1^{st} and 2^{nd} class frequency agile filter according to the value of $|A|$. This figure shows indeed the quadratic evolution of the frequency at 1^{st}-class leading to a slow increase of f_{0A1} according to $|A|$ while f_{0A2} increases much faster according to $|A|$ (linear theoretical equation). Therefore, all these simulation results allow verifying the above theory that we have introduced.

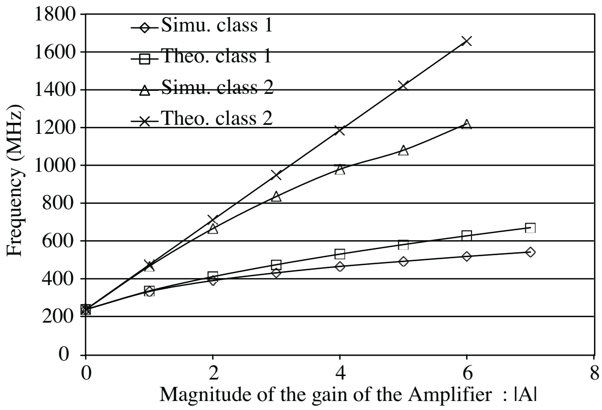

Figure 15. Theoretical and simulated values of f_0 and f_{0An} as a function of $|A|$ for the 1^{st} and 2^{nd}-class agile filter.

5.6. Description of the fabricated circuit

To fully validate the new approach, a zero-class filter and a 1^{st}-class agile filter were fabricated in a 0.25 μm SiGe BiCMOS technology from ST Microelectronics. Two different circuits were fabrication because of the limited number of available probes per one measurement operation. All circuits have been characterized in-situ using 50Ω RF voltage probes. To carry out the measurements, conversion circuits: voltage-current at the input and current-voltage at the output matched to 50 Ω and made from CCCII+ [48], have been added to the previous current mode filters in Figure 15 and Figure 16. The circuits were also biased under $\pm$2.5 V.

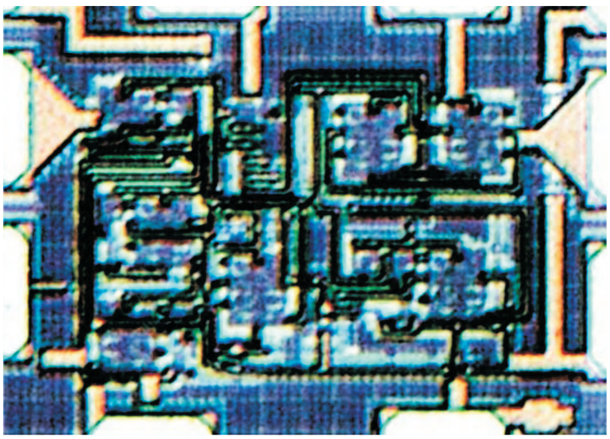

Figure 16. Die photograph of the frequency agile filter in 0.25 μm SiGe-BiCMOS technology.

Figure 16 shows the layout of the 1^{st}-class agile filter thus achieved. In this figure appear in part the pads where the measurement probes are laid. The total size of the circuit is $490 \times 400\ \mu\text{m}^2$ with pads and $300 \times 190\ \mu\text{m}^2$ without pads.

Figure 17 shows the measured frequency responses at $f_{0A1} = 1057$ and 1602 MHz for the agile filter when the bias currents $I_{01} = I_{02} = I_0$ are equal to 100 μA and that the current I_{0CR} is used to change the value of $|A|$. The values of $|A|$ were respectively: 2 and 5. The starting center frequency (zero-class filter) of 859 MHz that is greater than the frequency used for simulation results in Figure 18 is obtained for $A = 0$.

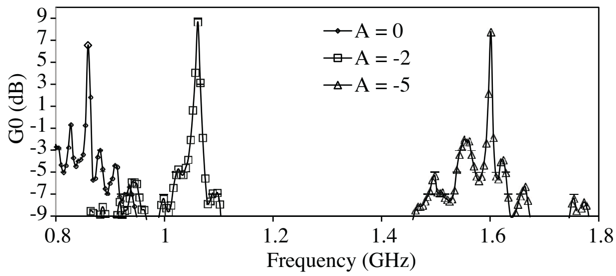

Figure 17. Frequency tuning measured results for some values of gain A.

Figure 17 shows the possibility of changing the center frequency f_{0A1} by changing the value of A and thus fully confirms the results obtained by simulation of Figure 14(a).

An agile filter at class 2 is currently being integrated.

5.6.1. Comparison with existent reconfigurable band pass filters

In Table 7 are reported the measurements results for our 1^{st}-class frequency agile filter. These results are compared to some recently published results for different types of reconfigurable band-pass filters implemented in various technologies. These results show that our filter in one of the few that are fully active. It does not include passive elements other than two capacitors, always necessary to make 2^{nd}-order active filters. Its bias voltage is low in comparison with ceramic filters [24]. Its chip size is one of the smallest and its power consumption is the lowest. Among active filter, this one also allows reaching the highest value of f_0 with the greatest flexibility of tuning.

6. Conclusions

In this article, we first of all recalled the principal definitions of the software radio and the ways of implementing it: multichannel receiver with elements in parallels or reconfigurable elements. The theoretical approach of Mitola which consists in digitizing the totality of the spectrum is beyond the state of the art of the ADC and moreover, because of supposed consumption, does not seem to be the best possible solution.

The cognitive radio which constitutes the most elaborate level of the software radio allows the adaptation of the system to its environment in order to be able to benefit best from totality of the available resources.

The encrypted communications which use the frequency hopping spread spectrum (FHSS) are mainly used in the military field. The frequency agility for these equipments is up to 500 MHz, frequency agile or reconfigurable filters are thus necessary.

Table 7. measurement results of the 1st-order agile filter compared to recently published measurement results of reconfigurable filters in various technologies. * *Measurements conducted without pads; ** conducted at 1.2 GHz.*

	Tsividis [31] 1996	Wu [40] 2003	Oualkadi [32] 2007	Entesari [48] 2007	Nakaska [30] 2007	Al-Ahmad [24] 2007	This work
Technology	0.8 µm BiCMOS	0.35 µm CMOS	0.35 µm CMOS	RF MEMS	0.18 µm CMOS	Ceramic	0.25 µm BiCMOS
Size	0.38 mm²	0.028 mm²	1.92 mm²	6000 mm²	2.8 mm²	8 4 mm²	0.057 mm²*
Kind of filter	Passive + Active	Active	Passive + Active	Passive	Passive + Active	Passive	Active
Tuning	Continuous	Continuous	Discret	Discrete	Continuous	Continuous	Continuous
# of passive elements	4	1	8	20	6	NA	2
f_{0max}	2 GHz	1.1 GHz	530 MHz	75 MHz	2.5 GHz	2.4 GHz	1.6 G Hz
f_{0max}/f_{0min}	1.25	2.75	2.2	3	1.38	3	2
Quality factor	350	80	300	60	5	850	400
Supply	3 V	2.7 V	3 V	0 – 90 V	1.8 V	200 V	± 2.5 V
consumption	24.4 mW	45.9 mW	57 mW	NA	37.8 mW	N/A	20 mW**

In the second part of this article, after having given the definitions of the frequency tuning range of a filter and having compared the concepts of tunable, reconfigurable and frequency agile filter, we made the state of the art of the various passive or active techniques which make it possible to obtain a tunable or reconfigurable filter. We compared their possibilities and showed that the active filters are those which up to 2.5 GHz present a greater ease of center frequency tuning. They are also completely integrated on current silicon technologies and require for their realization only very small silicon surface. Passive filters although having a good linearity are those which generally occupy most important silicon surfaces and are the least easily tunable.

All these limitations, then led us to the introduction of a new theory: the frequency agile active filters. Starting from a filter block with at least two outputs, band-pass and low-pass, we made a fully active agile filter. This filter makes use of a feedback amplifier. The center frequency of the agile filter is proportional to the gain A of this amplifier and therefore could be easily tuned over a wide frequency range. When the starting block includes the band-pass, low-pass and high-pass outputs they remain of the same type for the resulting agile filter.

The theory is thereafter generalized to the n^{th}-class. In the general case (n^{th}-class), the center frequency of the agile filter is given by $f_{0An} = (1-A)^n/2f_0$, where A is the gain of the required amplifiers and f_0 is the center frequency of the starting block (zero-class).

The simulation results presented for the 1^{st} and the 2^{nd} classes has fully confirmed the new theory introduced and highlighted its advantages. The measurements results carried out on the agile filter in current mode made from second-generation current controlled conveyors are also in perfect agreement with the above theory. These results were compared to previously published results, they emphasize the interest of our approach.

Our agile filter is one of the few to use a minimum number of passive elements. These 2^{nd}-order filters include the minimum required: two capacitors. It thus occupies a small silicon area and consumes the smallest power, while being tunable over a wide frequency range. Therefore, this new type of filter is a perfect candidate for cognitive and encrypted communications. For example, it will allow replacing a filter bank generally required in multiband receivers.

Acknowledgments

The authors would like to thank the support of STMicroelectronics for the realization of the integrated circuit and especially the interest for this work of Didier Belot.

References

[1] Pui-in Mak, Seng-Side U, Rui P. Martins “Transceiver structure selection: Review, State-of-the-art survey and case study,” IEEE Circuits and Systems Magazine, Vol. 7, Issue 2, 2007, pp. 6–25.

[2] Behzad Razavi, “RF Microelectronics,” Prentice Hall (1997), ISBN 978-0138875718.

[3] Yi-Ran Sun, “Generalized Bandpass Samplig Receivers for Software Defined Radio,” Doctoral Thesis, Royal Institute of Technology, ICT, Stockholm, Sweden, 2006.

[4] Mitola, J., “The software radio architecture,” IEEE Comm. Magazine, Vol. 33, No.5, May 1995, pp. 26–38.

[5] Abidi, A.A. “The Path to the Software-Defined Radio Receiver,” IEEE Journal of Solid-State Circuits, Vol. 42, Issue 5, May 2007, pp. 954–966.

[6] Mac Leod, J.R., Nesimoglu, T.; Beach, M.A., Warr, P.A., “Enabling technologies for software defined radio transceivers,” MILCOM 2002 Proceedings, Volume 1, 7–10 Oct. 2002, pp. 354–358.

[7] Maurer, L., Hueber, G., Dellsperger, T., Burger, T., Huemer, M, Weigel, R., “A frequency agile terminal receiver for wireless multi-standard applications,” IEEE Radio and Wireless Symposium, 17–19 Oct. 2006, pp. 291-294.

[8] Balwant Godara, “Conception of novel wideband performance-controllable RF circuits in SiGe : Impedance matching circuit, single-ended to differential baluns, and single-ended and differential low-noise amplifiers,” Doctoral thesis, IMS Lab., Bordeaux, France, November 2006.

[9] Cedric Majek, “Contribution a l’etude d’un Synthetiseur de Frequence pour Objets Communicants Multistandards en Technologie CMOS Soi,” Doctoral Thesis, IMS Lab. Bordeaux, France, October 2006.

[10] Mitola, J., Maguire, G. Q., Jr., “Cognitive radio: making software radios more personal,” IEEE Personal Communications, vol.6, no.4, August 1999, pp.13–18.

[11] Hella, M. M., “Overview: Trends and Implementation Challenges for Multi-Band/Wideband Communication,” Rensselaer Polytechnic Institute, April 2007, http://www.ecse.rpi.edu/Homepages/shivkuma/teaching/sp2007/wbn2007/wbn2007-hella-talk.ppt.

[12] http://en.wikipedia.org/wiki/Advanced_Encryption_Standard.

[13] http://en.wikipedia.org/wiki/RSA

[14] Andren, C., “A Comparison of Frequency Hopping and Direct Sequence Spread Spectrum Modulation for IEEE 802.11 Applications at 2.4 GHz,” 1997, http://www.intersil.com/design/prism/papers/ds-v-fh.pdf.

[15] http://www.reachinformation.com/define/Frequency-hopping_spread_spectrum.aspx.

[16] Robert K. Acherman "Software Enables Radio Family Ties," Signal Magazine September 2002, p. 31.

[17] Koochakzadeh, M., Tamijani, A., "Multi-scale tunable filter covering a frequency range of 6.5:1," Microwave Symposium Digest, 2008 IEEE MTT-S International, 15–20 June 2008, pp. 1023–1026.

[18] J. Brank, Z. J. Yao, M. Eberly, A. Malczewski, K. Varian, and C. L. Goldsmith, "RF MEMS-Based Tunable Filters," Int. J. of RF and Microwave CAE, vol. 11, no. 5, Sept. 2001, pp. 276–284.

[19] Arnaud Pothier, "Conception, Realisation Et Test De Microcommutateurs Micro-Electromecaniques Et Application Aux Circuits Hyperfrequences Reconfigurables," Doctoral Thesis, Xlim Lab., Limoges, France, December 2003.

[20] Ramachandran, D. Oz, A. Saraf, V.K. Fedder, G.K. Mukherjee, T., "MEMS-enabled reconfigurable VCO and RF filter," IEEE RFIC Symposium, 6–8 June 2004, pp. 251–254.

[21] El Hassan, M., Kerherve, E., Deval, Y., Belot, D., "A New Method to Reconfigure BAW-SMR Filters Using CMOS Transistors," IEEE/MTT-S International Microwave Symposium, 3–8 June 2007, pp. 1603–1606.

[22] Alexandre Augusto Shirakawa, "Étude, Synthèse Et Réalisations De Filtres Baw Pour Applications Mobiles," Doctoral Thesis, IMS Lab., Bordeaux, France, November 2006.

[23] Razafimandimby S., Tilhac C., Cathelin A., Kaiser A., Belot D., "A novel architecture of a tunable bandpass BAW-filter for a WCDMA transceiver," Analog Integrated Circuits and Signal Processing, Vol. 49, Issue 3, December 2006, pp. 237–247.

[24] Al-Ahmad, M., Matz, R., Russer, P., "0.8 GHz to 2.4 GHz Tunable Ceramic Microwave Bandpass Filters," IEEE MTT-S, 2007, pp. 1615–1618.

[25] Kim, Hyun-Suk; Hyun, Tae-Seon; Kim, Ho-Gi; Kim, Il-Doo; Yun, Tae-Soon; Lee, Jong-Chu, "Orientation effect on microwave dielectric properties of Si-integrated $Ba_{0.6}Sr_{0.4}TiO_3$ thin films for frequency agile devices," Applied Physics Letters, No. 89, 2006.

[26] Nosrati, M., Atlasbaf, Z., "A New Miniaturized Electronically Tunable Bandpass Filter, Antennas," 7th International Symposium on Propagation & EM Theory, ISAPE APOS'06, 26–29 October 2006, pp. 1–5.

[27] Karim, MF., Ai-Qun Liu, Alphones, A., Aibin Yu, "A Reconfigurable Micromachined Switching Filter Using Periodic Structures," IEEE Transactions on Microwave Theory and Techniques, Vol. 55, Issue 6, June 2007, pp. 1154–1162.

[28] Nath, J., Fathelbab, W., Franzon, P.D., Kingon, A.I., Ghosh, D., Maria, J.-P., Steer, M.B., "A tunable combline bandpass filter using barium strontium titanate interdigital varactors on an alumina substrate," IEEE MTT-S International Microwave Symposium, 2005, 12–17 June 2005, pp. 595–598.

[29] Carey-Smith, BE., Warr, PA., Beach, MA., "MEMS-driven flexible filters for cognitive radio," IST Mobile and Wireless Communications Summit, Dresden, Germany, June 2005, http://rose.bris.ac.uk/dspace/handle/1983/874.

[30] Dülger, F., Sánchez-Sinencio, E., Silva-Martinez, J., "A 1.3 V 5 mW fully integrated tunable bandpass filter at 2.1 GHz in 0.35-μm CMOS," IEEE journal of Solid-State Circuits, vol. 38, No 6, 2003, pp. 918–928.

[31] Pipilos, S., Tsividis, Y.P., Fenk, J., Papananos, Y., "A Si 1.8 GHz RLC filter with tunable center frequency and quality Factor," IEEE journal of Solid-State Circuits, vol. 31, No 10, 1996, pp. 1517-1525.

[32] Biolek, D., Biolkova, V., Kolka, Z., “Universal Current-Mode OTA-C KHN Biquad,” International journal of Electronics, Circuits and Systems Vol. 1, No 4, pp. 214–217.

[33] Biolek, D., Biolkova, V., Kolka, Z. “Universal current-mode Gm-C biquad,” 18th International Conference Radioelektronika, Prague, Czech Republic, 24–25 April 2008, pp. 1–3.

[34] Lin, P.M., “Signal Flow Graph In Filter Analysis And Synthesis,” Circuits and Filters Handbook, Chap. 18, IEEE Press 1995, pp. 619–638.

[35] Ngamkham, W. Pawarangkoon, P. Kiranon, W “A novel noninteracting Electronically Tunable Universal Filter,” International Symposium on Communications and Information Technologies, ISCIT ’06. Oct. 2006, pp. 843–846.

[36] Chunhua Wang , Haiguang Liu, Yan Zhao, “A New Current-Mode Current-Controlled Universal Filter Based on CCCII(±),” Circuits, Systems, and Signal Processing, Birkhäuser Boston, Vol. 27, No. 5, October 2008, pp. 673–682.

[37] El Oualkadi, A.E., El Kaamouchi, M., Paillot, J.-M., Vanhoenacker-Janvier, D., Flandre, D., “Fully Integrated High-Q Switched Capacitor Bandpass Filter with Center Frequency and Bandwidth Tuning,” IEEE Radio Frequency Integrated Circuits (RFIC) Symposium, 3–5 June 2007, pp. 681–684.

[38] Cheung, Vincent S.L., Luong, Howard Cam H., “Design of Low-Voltage CMOS Switched-Opamp Switched-Capacitor Systems,” The Springer International Series in Engineering and Computer Science, Vol. 737, 2003, ISBN: 978-1-4020-7466-0.

[39] Seng-Pan U, Rui Paulo Martins, José Epifânio da Franca. “Design of Very High-frequency Multirate Switched-capacitor Circuits: Extending the Boundaries of CMOS Analog Front-end Filtering,” Springer, 2006 ISBN 0387261214, 9780387261218.

[40] Mariano A., Goumballa B., Dallet D., Deval Y., Begueret, J-B., “Design of a high-speed CMOS multi-bit quantizer for continuous-time Delta-Sigma Modulator applications,” Analog Integrated Circuits and Signal Processing, vol. 57, No. 1-2, November 2008, pp. 79–87.

[41] Yue Wu, Chunlei Shi, Xiaohui Ding, Ismail, M., Olsson, H., “Design of CMOS VHF/RF Biquadratic Filters,” Analog Integrated Circuits and Signal Processing, Vol. 33, Issue 3, December 2002, pp. 239–248.

[42] Zhiqiang Gao, Mingyan Yu, Yizheng Ye, Jianguo M “A CMOS bandpass filter with wide-tuning range for wireless applications,” Proceedings ISCAS 2006, pp. 867–870.

[43] Stornelli, V., Ferri, G., Leuzzi, G., De Marcellis, A., “A Tunable 0.5–1.3 GHz CMOS 2nd order Bandpass Filter with50 Ω Input-output Matching Impedance,” Proceedings ISCAS 2006, pp. 863-866.

[44] Multi-Projets website : http://cmp.imag.fr.

[45] Fabre, A., Saaid, O., Wiest, F., Boucheron, C., “High frequency applications based on a new current controlled conveyer,” IEEE Transaction on Circuits and Systems, vol. 43, February 1996, pp. 82–91.

[46] Fabre, A., Saaid, O., Wiest, F., Boucheron, C., “Low Power Current-Mode Second-Order Bandpass IF Filter,” IEEE Transactions On Circuits And Systems—II: Analog And Digital Signal Processing, Vol. 44, No. 6, June 1997, pp. 436–446.

[47] Salem, S., Fakhfakh, M., Masmoudi, D, Loulou, M., Loumeau, P., Masmoudi, N., “A high performances CMOS CCII and high frequency applications,” Analog Integrated Circuits and Signal Processing, Vol. 49, Number 1, October 2006, pp. 71–78.

[48] Fabre, A, Saaid, O., Wiest, F., Boucheron, C., “High Frequency High-Q BiCMOS Current-Mode Bandpass Filter and Mobile Communication Application,” IEEE Journal Of Solid-State Circuits, Vol. 33, No. 4, April 1998, pp. 614–625.